

**Power capacity profile estimation for
building heating and cooling in
demand side management**

J. A. Gomez

M. F. Anjos

G-2016-75

September 2016

Cette version est mise à votre disposition conformément à la politique de libre accès aux publications des organismes subventionnaires canadiens et québécois.

Avant de citer ce rapport, veuillez visiter notre site Web (<https://www.gerad.ca/fr/papers/G-2016-75>) afin de mettre à jour vos données de référence, s'il a été publié dans une revue scientifique.

This version is available to you under the open access policy of Canadian and Quebec funding agencies.

Before citing this report, please visit our website (<https://www.gerad.ca/en/papers/G-2016-75>) to update your reference data, if it has been published in a scientific journal.

Les textes publiés dans la série des rapports de recherche *Les Cahiers du GERAD* n'engagent que la responsabilité de leurs auteurs.

La publication de ces rapports de recherche est rendue possible grâce au soutien de HEC Montréal, Polytechnique Montréal, Université McGill, Université du Québec à Montréal, ainsi que du Fonds de recherche du Québec – Nature et technologies.

Dépôt légal – Bibliothèque et Archives nationales du Québec, 2016
– Bibliothèque et Archives Canada, 2016

The authors are exclusively responsible for the content of their research papers published in the series *Les Cahiers du GERAD*.

The publication of these research reports is made possible thanks to the support of HEC Montréal, Polytechnique Montréal, McGill University, Université du Québec à Montréal, as well as the Fonds de recherche du Québec – Nature et technologies.

Legal deposit – Bibliothèque et Archives nationales du Québec, 2016
– Library and Archives Canada, 2016

Power capacity profile estimation for building heating and cooling in demand side management

Juan A. Gomez
Miguel F. Anjos

*GERAD & Department of Mathematics and Industrial
Engineering, Polytechnique Montréal (Québec) Canada,
H3C 3A7*

juan.gomez@polymtl.ca
miguel-f.anjos@polymtl.ca

September 2016

Les Cahiers du GERAD
G-2016-75

Copyright © 2016 GERAD

Abstract: This paper presents a new methodology to estimate power capacity profiles for smart buildings. The capacity profile can be used within a demand side management system in order to guide building temperature operation. It provides a trade-off between the quality of service perceived by the end user and the requirements from the grid in a demand response context. A data fitting approach and a multiclass classifier are used to compute the required profile to run a set of electric heating and cooling units via an admission control module. Simulation results are reported to validate the performance of the proposed methodology under different conditions, and a comparison made with neural networks in a real world-based scenario.

Keywords: Smart buildings, power demand, residential load sector, least squares, parameter estimation, classification

Acknowledgments: This research was supported by the *Canada Research Chair on Discrete Nonlinear Optimization in Engineering*.

1 Introduction

In the context of power systems, reducing peaks and the fluctuation of consumption brings stability to the system and benefits to the players along the power supply network. In this respect, demand response programs (DR) and demand side management (DSM) systems encourage and facilitate the participation of the end users in the grid decisions. This participation is increasing with the development and implementation of smart buildings. Although DR programs have mostly been oriented to large consumers, these smart buildings will allow to exploit the DR potential in residential and commercial buildings as well. These represent around 70% of the total energy demand in the United States [1]. In Canada, space heating is responsible for more than 60% of the total residential energy consumption due to the cold climate [2]. Across the country electric baseboards account for the 27% of the heating equipments, reaching 66% in the province of Quebec. On the other hand, the province of Ontario is typically a summer-peaking region due to the high temperatures during that season and the high penetration of air conditioning systems [3, 4].

Different DSM-related works have been published by several authors. Normally their research motivation is oriented to the management of loads, user behavior, cost performance and curve shaping. Fixing a capacity constraint is a common idea among these approaches. The multi-layer architecture presented in [5] proposes a scheme for online operation and control of different types of loads given a maximum consumption level. In the same way, a capacity constraint is imposed by a DR aggregator in the stochastic DSM program in [6]; bidding curves and price analysis are reported in order to guide end users about increasing their capacities. In [7] the authors evaluate the performance of several heuristic-based controllers. They define the load management as a knapsack problem with preset power capacities per time slot. In a similar way, [8] assumes a consumption limit that only allows to activate one load at a time. The idea of capacity subscription is explored in [9] where the individual consumer's demand is limited in a competitive market. On the other hand, the heuristic algorithm proposed in [10] aims to minimize the error between the actual power consumption and the objective load curve by moving the shiftable loads. In this case the objective load curve can be seen as a soft constraint capacity profile.

All of approaches mentioned represent the capacity as a given parameter and some of them recognize the importance of a forecasting tool to determine how that capacity should be. At this point, estimating the user consumption is a key step to facilitate decision-making process for users as well as for higher levels in the power system.

Works have been published specifically in load forecasting related areas. A comprehensive review of forecasting methods from classical time series to more sophisticated machine learning tools is given in [11].

Load estimation methods are classified depending on the level of aggregation of the input data; those can be bottom-up or top-down models [12]. Bottom-up models extrapolate the behavior of a larger system based on its inner elements. Top-down models make decisions from a global perspective and share it among all the subsystems.

Notation	
$h \in \{1, 2, \dots, H\}$	Set of time frames in horizon.
$t \in \{1, 2, \dots, S\}$	Set of time steps in time frame h .
$i \in \{1, 2, \dots, I\}$	Set of loads.
N_h	Number of requests received in time frame h .
P_i	Power consumption of appliance i .
C_h	Power capacity in time frame h .
x_{it}	$\begin{cases} 1 & \text{if request from } i \text{ is accepted in time step } t \\ 0 & \text{Otherwise} \end{cases}$
QoS_h	Quality of service in time frame h .
\tilde{QoS}_h	Quality of service of the prediction model in time frame h .
T_h	External temperature in time frame h .
\mathcal{P}	Power consumption of the loads in each scenario.
Ω	Discrete set of capacities.
$\omega \in \Omega$	Capacity class.

Within these two categories we can find different approaches that have been used to estimate energy demand. Artificial Neural Network and Auto Regressive Integrated Moving Average are compared in [13] showing the effect on the scheduling of storage devices. An approach using support vector regression is presented in [14] evaluating the impact of the time and space granularity inside a multi-family unit.

Logistic and Poisson regression are used in [15] to estimate energy demand in a large aggregated population. In a similar way, [16] presents a short-term forecasting method for aggregated loads, specifically in buildings with daily or seasonal patterns of consumption. On the other hand, when the prediction output belongs to a discrete set of categories it is defined as a classification problem. Some related energy problems can be treated this way: price forecasting in [17] and wind power ramp events in [18].

This paper proposes an approach to estimate a power capacity profile that works in combination with the admission controller (AC) module presented in [5]. This profile is used to ensure enough power to meet the demand for the next planning horizon (e.g. the next day in a day-ahead DR market). Estimating the capacity that will be necessary allows to define a relationship between the total expected demand and the level of service the user desires while providing DR. In this scenario the user will book a variable maximum power consumption over the planning horizon ensuring a pre-established level of service. This approach could also include external factors such as peak control and pricing policies. The motivation is that having a defined power *budget* limits the consumption and encourages load shifting. It also facilitates the integration of differential pricing for both energy and power.

This paper is structured as follows. The proposed methodology is described in Section 2. Simulation results for the real world-based scenario is presented in Section 3, and conclusions are discussed in Section 4.

2 Power capacity profile

Figure 1 shows the application of the AC module presented in [5]. The space heaters and the air conditioners are able to create requests at time step t when the room temperature is going out of the thermal comfort zone. The online algorithm in the AC sorts all the requests based on a priority value that is a function of the external and internal temperatures. The AC accepts or rejects the requests sent by each appliance given the previous ordering and a defined capacity C_h for the whole time frame. Finally it sends the signal x_{it} back to each smart appliance i either to run or to stand by for the next time step.

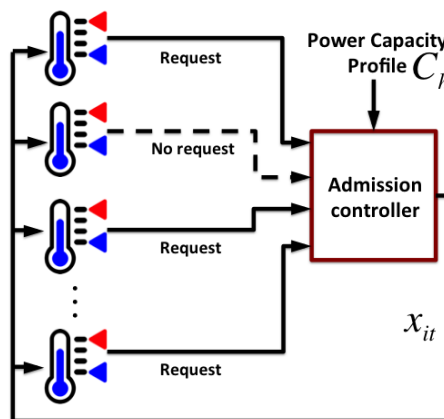


Figure 1: Admission controller

Figure 2 presents a basic example of the AC operation. A smart house with two rooms, R1 and R2, is simulated over a horizon of 5 time frames. Each time frame is composed by 10 time steps where the smart loads can send requests. Typically a time frame would be equivalent to an hour in a realistic scenario. There is a 1.5 kW space heater in each room and the external temperature is 5°C, Figure 2(a).

We can see the peak reduction obtained by the AC in Figure 2(b); the end-user agrees to have a preset power capacity (dashed red line) which constrains the consumption up to 1.5 kW. The peak of consumption,

for this example 3kW, would be attained when the two space heaters are being used at the same time step. Figures 2(c) and 2(d) show the internal temperature in each room within a certain comfort zone. In a similar way, we can see the time steps where the heaters are working in Figures 2(e) and 2(f). For more details about the AC algorithm and the heat transfer equations we refer the reader to [5].

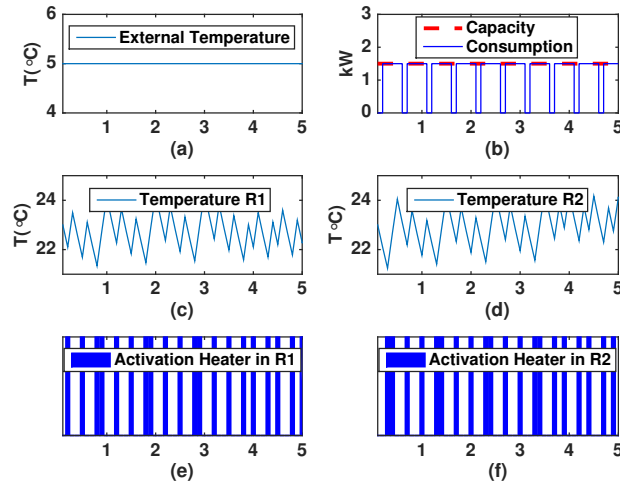


Figure 2: Example of results from admission controller

In the previous example the capacity profile is enough to keep the internal temperature in the comfort zone and to achieve a peak shaving effect. However, alternating the use of the heaters might not be enough to ensure a comfortable internal temperature if the external temperature is extremely cold; a higher capacity profile might be required. This decision becomes more complex if we increase the number of space heaters and if those loads have different power consumption.

We introduce the Quality of Service (QoS) index to quantify the impact of a given capacity C on the whole system. The general idea of QoS is that the user should be willing to pay more if a higher level of service is desired. This decision-making by the user is especially important under time-of-use pricing conditions because the customer can profit from the lower price time frames by reshaping the load curve while ensuring the desired QoS .

In a smart building it is possible to compute the QoS from the information provided by thermostats and smart appliances connected to the AC. In the same spirit as in [19], we define the QoS in each time frame h as follows:

$$QoS_h = \begin{cases} \frac{\sum_{i=1}^I \sum_{t=1}^S x_{it}}{N_h} \times 100\% & N > 0 \\ 100\% & N = 0. \end{cases} \quad (1)$$

The accepted requests have to satisfy

$$\sum_{i=1}^I x_{it} P_i \leq C_h \quad \forall t \in \{1, 2, \dots, S\}. \quad (2)$$

Equation (2) represents how the AC accepts requests until the capacity limit is reached. In the framework of this article we assume that both air conditioning units and electric baseboards heaters have a constant level of consumption [20]. Let $C_h \in \Omega$, where Ω is a set of capacities that are suitable to work in combination with the admission controller and the set of loads. In other words, we do not want a capacity to operate a fractional number of loads in the time step t . Given that Ω is a discrete set we can define the classification problem

$$\Phi(T_h, QoS_h) = C_h \quad (3)$$

that determines $C_h \in \Omega$ for given external temperature T_h and the QoS_h defined by the user. We solve this classification problem with a three step approach: selection of the training set from historical data, function fitting and final classification. We illustrate the steps in this section with a group of space heaters; Section 3 includes experimental results for both type of loads.

2.1 Sampling from historical data

The real data is obtained from the smart energy management system, which records the accepted requests, the rejections and the evolution of the quality of service over time. In this article we simulate this historical data to understand the system's dynamics and to implement a prediction model. The simulation conditions are:

- The set of heaters is composed of four identical units of 1.5 kW of consumption.
- The heat transfer is computed by using the specific heat and Fourier's law formulations implemented in [5].
- The external temperature corresponds to the complete year 2013 (8760 hours) in the Montreal area [21].
- The comfort interval for the internal temperature is $[22 - 24]^\circ\text{C}$.
- C_h is randomly chosen from $\Omega = [1.5, 3.0, 4.5, 6.0]$ based on the interval of temperature (the highest capacities are not necessary during the warmer days).

Figure 3 shows the frequency of the external temperature intervals in the historical data; this is clearly an imbalanced set. This imbalance is generated by the similar weather in Spring and Fall. The temperatures between 0 and 20°C would have a significantly higher weight in a fitting process. We use random under-sampling [22] in order to match the number of points in the minority group from the temperatures below the comfort interval.

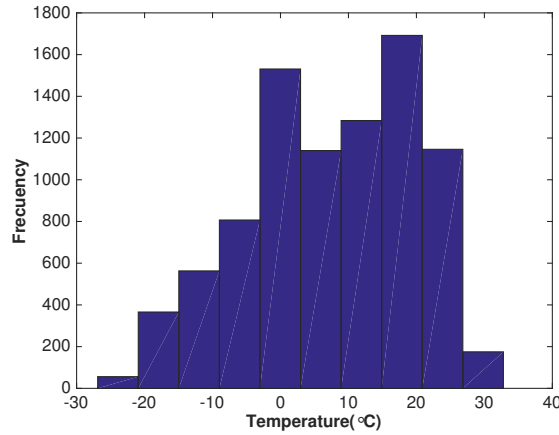


Figure 3: Histogram of hourly external temperatures in Montreal, Canada for 2013

The hourly QoS results for the balanced set data are shown in Figure 4. We can identify several characteristics of the system behavior:

- As the temperature increases the QoS converges to higher values; with fewer requests the selection of a capacity level is a less sensitive issue.
- The selection of the capacity level has a big impact on the QoS in lower temperature conditions.
- The QoS seems to behave asymptotically for higher and lower temperatures.

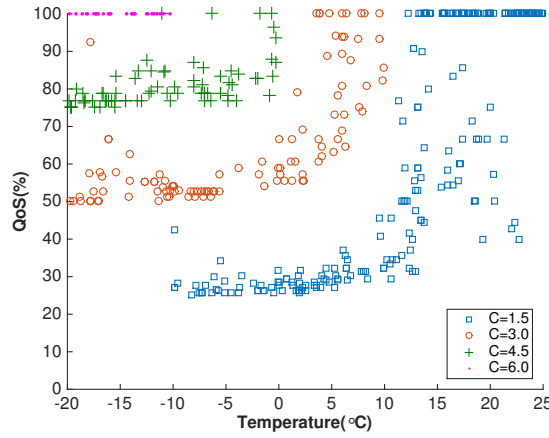


Figure 4: Graph of QoS vs temperature for the sampled historical data

2.2 Data fitting

Once we have identified these features in the data set we can solve an optimization problem for the capacity estimation. We propose to fit the sigmoid function

$$\widehat{QoS}_h = \frac{\beta_1}{1 + e^{\beta_2 T_h}} + \beta_3 C_h + \beta_4, \quad (4)$$

where \widehat{QoS}_h is the quality of service from the prediction model at time frame h .

Additionally we will compare two different optimality criteria: least squares value (LSV) and least absolute value (LAV). Typically LSV gives more weight to further points while the LAV is resistant to outliers [23].

The optimization problems are:

$$\min_{\beta_1, \beta_2, \beta_3, \beta_4} \sum_H (QoS_h - \widehat{QoS}_h)^2 \quad (5)$$

$$\min_{\beta_1, \beta_2, \beta_3, \beta_4} \sum_H |QoS_h - \widehat{QoS}_h| \quad (6)$$

The results for a least-squares fitting of a sigmoid function can be seen in Figure 5.

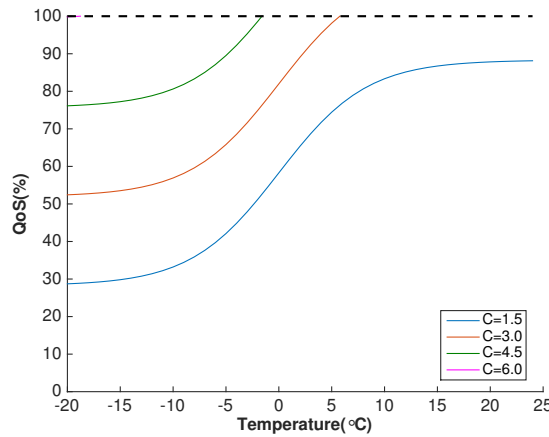


Figure 5: Fitted sigmoid function

Once we have solved the optimization problem (5) or (6) we can use (4) to compute the expected required capacity for the desired quality of service.

2.3 Motivation for using a sigmoid function

The selection of a sigmoid function not only has a graphic justification but also a more interesting background. We provide intuition into why it works for the heating case; the cooling case is similar.

We make the following assumptions:

- If $T' < \hat{T}$ then $N(T') > N(\hat{T})$ for any temperatures T' and \hat{T} .
- $C \in [C_{\min}, \infty)$ where $C_{\min} = \max(P_i)$.
- Each appliance generates at most one request per time step, therefore the maximum number of requests per step equals I .
- There exists a temperature \tilde{T} at which all the heaters generate requests at every time step, therefore $N(\tilde{T}) = I \times S$.

By looking at the worst-case scenario for any time frame in equations (1) and (2):

$$QoS(\tilde{T}, C_{\min}) = \frac{\sum_{i=1}^I \sum_{t=1}^S x_{it}}{I \times S} \quad (7)$$

$$\sum_{i=1}^I x_{it} P_i \leq C_{\min} \quad \forall t \in \{1, 2, \dots, S\} \quad (8)$$

Equation (8) allows to accept at least one request at every time step. Therefore the total number of accepted requests satisfies:

$$\sum_{t=1}^S \sum_{i=1}^I x_{it} \geq S. \quad (9)$$

After replacing (9) in (7) we can obtain a minimum QoS :

$$QoS(\tilde{T}, C_{\min}) \geq \frac{1}{I} \quad (10)$$

We can see a similar behavior for scenarios with temperature $\dot{T} > \tilde{T}$ and $N(\dot{T}) < N(\tilde{T})$. Let F be the minimum number of time steps where requests are received. Knowing that each appliance i will only request at most once per time step:

$$F = \left\lceil \frac{N(\dot{T})}{I} \right\rceil = \frac{N(\dot{T})}{I} + \alpha, \quad 1 > \alpha \geq 0. \quad (11)$$

The variable F also becomes the minimum number of accepted requests due to the C_{\min} in equation (8). By replacing (11) in (1) we obtain:

$$QoS(\dot{T}, C_{\min}) = \frac{\sum_{i=1}^I \sum_{t=1}^S x_{it}}{N(\dot{T})} \geq \frac{F}{(F - \alpha)I}. \quad (12)$$

When $\alpha = 0$ we get the same condition as in equation (10).

A sigmoid function helps to represent asymptotic extremes and monotonic behavior of the QoS . In the first case, we see how the QoS is bounded below in equations (10) and (12), and bounded above by definition ($QoS \leq 100$). In the second case, temperature and requests are inversely proportional (if $T' < \hat{T}$ then $N(T') > N(\hat{T})$), therefore $QoS(T)$ is monotonically increasing. Using a linear function would capture the monotonic condition but not the asymptotic extremes.

For cooling systems we would change the first assumption to $T' > \hat{T}$ then $N(T') > N(\hat{T})$, obtaining a similar monotonically decreasing sigmoid function over the interval of external temperature where cooling is required.

2.4 Classification

As stated previously, we have a discrete set of capacities that are suitable for the performance of the system. We solve for C_h in (4) in order to compute the continuous signal \widehat{C}_h . Finally we use the multiclass classifier

$$C_h = \arg \min_{\omega \in \Omega} | \widehat{C}_h - \omega | \quad (13)$$

to find the required capacity.

In Figure 6 we see the effect of the classifier; it assigns areas to each one the capacities based on the mid-points between each pair of sigmoid curves from Figure 5.

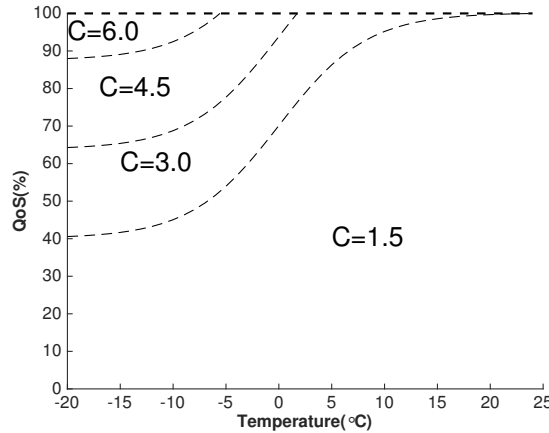


Figure 6: Classification areas

3 Experimental results

In the previous section we introduced the methodology with an example for a given set of homogeneous space heaters. In this section we carry out several experiments to assess and validate the performance under different conditions. We define a building with a comfort zone of $[22 - 24]^{\circ}\text{C}$. For a more realistic scenario both type of loads will be managed by the AC; the space heaters and the air conditioners will create requests when the temperature in each room is going below and above the comfort zone respectively.

The experiments include:

- Sets \mathcal{P} with homogeneous and heterogeneous power consumption P_i values.
- Three different types of Ω sets: computed from all possible combinations of values in \mathcal{P} ; from some of the combinations in \mathcal{P} ; and Ω given by an external entity.
- Two fitted functions.
- Two optimality criterion: LAV and LSV.
- Comparison with two neural networks with different topology.

The experiments are carried out in two stages. First in the training stage we reproduce the approach presented in Section 2 in order to determine the classification areas. Subsequently in the test stage we use the classification areas to estimate the capacity profiles for given QoS . Once the profiles are computed, we run a simulation to verify the actual QoS performance.

3.1 Training

We required two training sets; one for heaters and one for air conditioners. Each training set is defined over the corresponding interval of temperature ($T_h \leq 22^{\circ}\text{C}$ for heaters and $T_h \geq 24^{\circ}\text{C}$ for air conditioners)

and randomly chosen as in Subsection 2.1. The historical sets are simulated with the hourly temperature in Montreal for the year 2013 (8760 data points).

As mentioned before, we will compare this methodology with other two approaches. In the first case, we use the polynomial function

$$\widehat{QoS}_h = \beta_1 + \beta_2 C_h + \beta_3 T_h + \beta_4 T_h C_h \quad (14)$$

instead in the fitting step. A priori the sigmoid function gives a better representation of the historical set due to its monotonically increasing behavior and the asymptotic extremes. The function in Equation (14) captures only the monotonic condition.

We will use neural networks (NNs), a widely used method in many different types of problems, as a second benchmark. For classification problems the NNs typically have the same number of neurons in the output layer as the number of classes. The NN computes the probability that each input belongs to each class; finally it chooses the class with maximum probability. In this case we implemented two NNs with $A = 1$ and $B = 2$ hidden layers (5 neurons each), cross entropy as a performance measure in the learning process and a validation subset of 30% of the points.

Finally the total confusion or missclassification index will allow to compare the performance of each one of approaches. It shows the percentage of the total set of data that was incorrectly classified.

Tables 1 and 2 show the training results for the different scenarios and approaches. Scenarios (1 – 7) and scenarios (8 – 14) correspond to heating and cooling respectively. In scenarios (1 – 3) and (8 – 10) the loads are homogeneous and the Ω set correspond to all possible combinations of the loads. In scenarios (4 – 6) and (11 – 13), both homogeneous and heterogeneous loads are tested with a Ω set that was defined separately from the loads. Finally scenarios 7 and 14 contain a heterogeneous set of loads and all possible combinations in Ω .

Table 1: Confusion (%) in training stage for the heaters scenarios

Scenario	\mathcal{P}	Ω	<i>PLAV</i>	<i>PLSV</i>	<i>SLAV</i>	<i>SLSQ</i>	NN_A	NN_B
1	[1.5, 1.5, 1.5]	[1.5, 3.0, 4.5]	15.14	14.26	13.84	14.17	16.80	16.90
2	[2.0, 2.0, 2.0]	[2.0, 4.0, 6.0]	18.65	21.82	15.07	10.71	4.06	16.57
3	[2.5, 2.5, 2.5]	[2.5, 5.0, 7.5]	20.83	22.02	23.41	15.67	13.99	14.18
4	[1.5, 1.5, 1.5]	[2.5, 4.0, 6.0]	37.69	36.31	15.48	15.80	7.34	15.67
5	[2.0, 2.0, 2.0]	[2.5, 4.0, 6.0]	22.42	26.78	18.25	13.88	15.67	15.67
6	[2.5, 2.0, 1.5]	[2.5, 4.0, 6.0]	20.64	21.32	7.14	8.33	10.42	10.21
7	[2.5, 2.0, 1.5]	[2.5, 3.5, 4.0, 4.5, 6.0]	42.85	50.59	33.33	43.65	21.62	16.07

Table 2: Confusion (%) in training stage for the cooling scenarios

Scenario	\mathcal{P}	Ω	<i>PLAV</i>	<i>PLSV</i>	<i>SLAV</i>	<i>SLSV</i>	NN_A	NN_B
8	[0.5, 0.5, 0.5]	[0.5, 1.0, 1.5]	15.03	19.68	13.35	11.19	16.36	19.8
9	[1.0, 1.0, 1.0]	[1.0, 2.0, 3.0]	21.41	17.91	19.19	16.54	11.74	18.44
10	[1.5, 1.5, 1.5]	[1.5, 3.0, 4.5]	21.49	19.29	18.66	11.09	16.41	11.27
11	[0.5, 0.5, 0.5]	[1.5, 2.0, 3.0]	18.72	20.54	18.19	12.66	12.94	17.11
12	[1.0, 1.0, 1.0]	[1.5, 2.0, 3.0]	21.01	18.63	17.11	18.25	11.56	11.07
13	[1.5, 1.0, 0.5]	[1.5, 2.0, 3.0]	21.81	13.31	13.31	15.99	11.78	14.45
14	[1.5, 1.0, 0.5]	[1.5, 2.0, 2.5, 3.0]	22.01	24.54	24.40	20.86	17.81	16.97

In general we observe a better performance in the sigmoid fitting (*SLAV* and *SLSV*) than in the polynomial cases (*PLAV* and *PLSV*). There is no clear difference in terms of the fitting criterion. The sigmoid function seems to be competitive with both NNs in the first six scenarios of each table.

As stated before, the sigmoid function makes a better representation of the structure of the problem. Figure 7 shows the classification areas obtained by fitting the sigmoid and the polynomial function for the scenario 2. For a QoS of 90%, we see that the polynomial function gives a transition between areas either

before or after the sigmoid function. If it is before, $T \in (-18, -12)^\circ\text{C}$, we will obtain a worse QoS and lower temperatures in the rooms. If it is after, $T \in (-2, -8)^\circ\text{C}$, we will have extra capacity that it is not required.

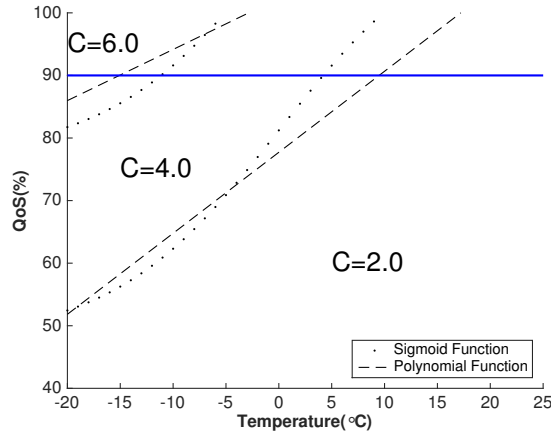


Figure 7: Comparison sigmoid and polynomial functions for scenario 2

On the other hand, scenarios 7 and 14 present a significant difference: the NNs have a considerable better performance than any other approach. Looking deeper into the characteristics of these scenarios we realize a special condition: several values in Ω can generate the same QoS at the same temperature. We may have the exact same performance in scenario 7 for $\omega = 4$ and $\omega = 4.5$ if the three heaters send requests at the same time. In the first case, the AC will accept P_1 and P_3 and leave P_2 for the next time step. In the second case the order of acceptance changes but the QoS remains equal. Figure 8 shows the training set for this scenario; we can see how $C = 4$ is distributed over its adjacent classes.

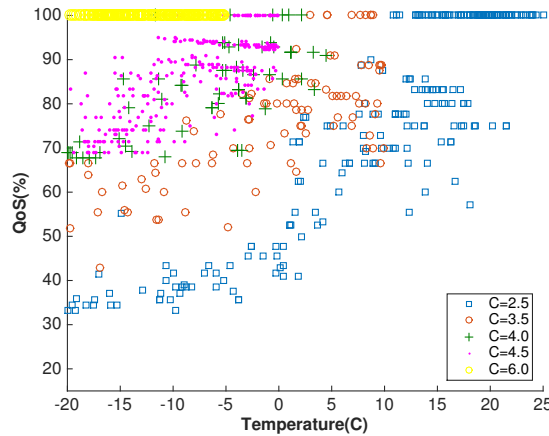


Figure 8: Training data for scenario 7 (Heaters)

Although the NNs have a better training performance, they might minimize the confusion value by eliminating one of the classes. Let W_ω the set of points that belong to class ω and W_ω^1 and W_ω^0 the subsets of points correctly and incorrectly classified respectively. Let Γ be the total number of misclassified points. The approach presented in this article separates any two contiguous sets following the fitted function, therefore: $W_1^1 + W_1^0 = |W_1|$, $W_2^1 + W_2^0 = |W_2|$ and $W_1^0 + W_2^0 = \Gamma$.

If we assume that the NN eliminates class 2: $\bar{W}_1^1 = |W_1|$, $\bar{W}_2^0 = |W_2|$ and $W_2^1 + W_2^0 = |W_2| = \bar{\Gamma}$. Consequently we can conclude that eliminating one class improves the confusion (i.e. $\bar{\Gamma} < \Gamma$) if $W_2^1 < W_1^0$.

At this point we can foresee the advantage of exploiting the features of the problem. In the approach presented in this paper the fitted function acts as a constraint that represents the structure of the data sets. On the other hand, the flexibility of the NNs allows a lower misclassification but we see in the Subsection 3.2 that this has an unexpected impact on the QoS .

3.2 Test

The test experiments are carried out over a period of two years (2014 and 2015) for the Montreal area (17520 data points). The user sets a QoS of 90%. Figures 9 – 14 show the results for scenarios 2 and 7 (heaters) and scenario 14 (cooling). These box plots contain the minimum value, the maximum value and interquartile range for the hourly QoS and the hourly average temperature in the three rooms for each one of the methods compared.

For scenario 2 (Figures 9 and 10) we see that the sigmoid and the NNs cases perform better than the polynomial function. This behavior is consistent with the training results in the previous subsection. Scenarios 1, 3 – 6 and 8 – 13 showed similar results.

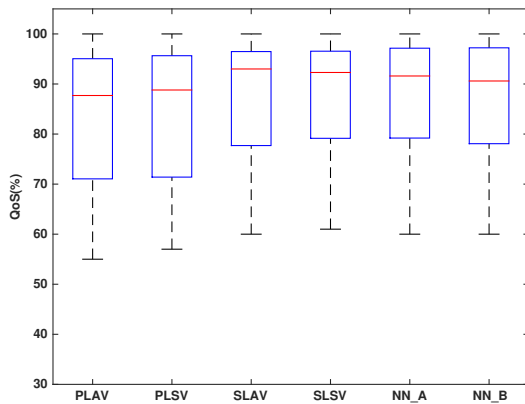


Figure 9: QoS test results for scenario 2 (Heaters)

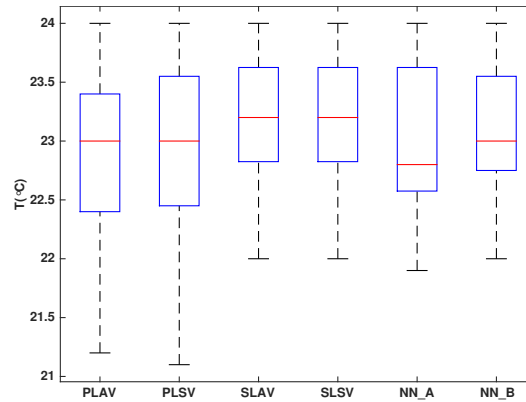


Figure 10: Average room temperature test results for scenario 2 (Heaters)

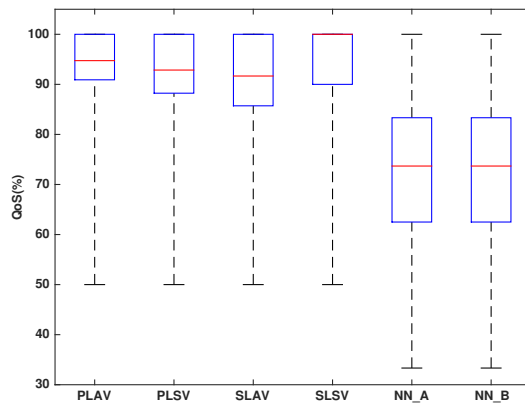


Figure 11: QoS test results for scenario 7 (Heaters)

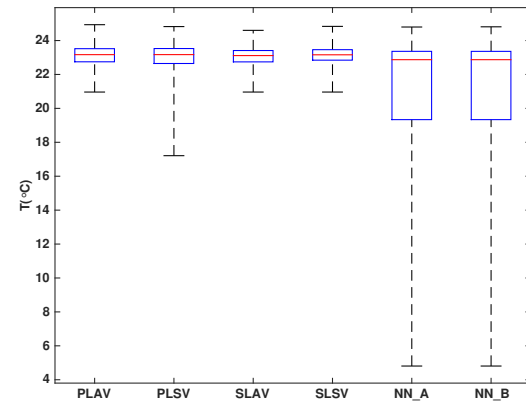


Figure 12: Average room temperature test results for scenario 7 (Heaters)

In the case of scenarios 7 and 14 we observe a particular situation: although the training results for NNs are better we have a worse QoS (Figures 11 and 13) and temperature management (Figures 12 and 14). We previously saw in Figure 8 how the areas for classes 3.5, 4 and 4.5 were not clearly defined. We also saw how different capacities could result in a similar QoS at the same temperature due to the load shifting. Nevertheless eliminating one of the classes can have negative effects on the final output; in this case the NNs tend to eliminate class 4.5 in order to minimize the confusion value. Although $C = 4.5$ and $C = 4.0$ can accept two out of the three loads if all of them arrive at the same time, the situation changes when the loads arrive at different times. For example, $C = 4.5$ will satisfy any of the combinations of two loads arriving simultaneously: $[2.0, 2.5]$, $[1.5, 2.5]$ and $[1.5, 2.0]$, whereas $C = 4.0$ will not accept $[2.0, 2.5]$. In that sense it is preferable not to eliminate a class because of the dynamics in the system.

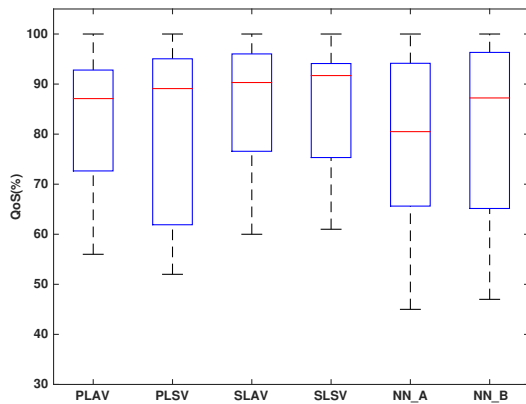


Figure 13: QoS test results for scenario 14 (Cooling)

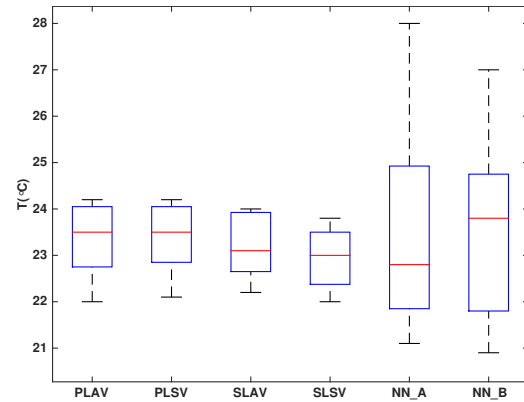


Figure 14: Average room temperature test results for scenario 14 (Cooling)

4 Conclusions

Understanding the requirements of residential consumption is a key element to facilitate increased participation in demand response programs. The methodology proposed in this paper computes a power capacity profile that meets the user's expectations and at the same time provides information to residential power management systems. The use of the admission controller and implementation of the quality of service index allow to aggregate a set of loads simplifying the making decision process.

The approach presented in this paper profits from the inner structure of the defined problem ensuring a good representation of the historical data and a reliable tool for the future estimation. The shaving effect can be achieved, controlling the peak consumption, respecting the QoS and ensuring a better utilization of the power capacity available.

Finally, the approach presented is computationally efficient, it utilizes data that is normally available in the smart building context, and performs well for heating and cooling, offering a better performance than neural networks in a real world-based scenario.

References

- [1] Electric Power Annual 2014, Tech. rep., U.S Energy Information Administration (2016).
- [2] Households and the Environment: Energy Use, Tech. rep., Statistics Canada (2013).
- [3] 2014 Yearbook of Electricity Distributors, Tech. rep., Ontario Energy Board (2015).
- [4] Survey of Household Energy Use, Tech. rep., Natural Resources Canada (2011).
- [5] G. T. Costanzo, G. Zhu, M. F. Anjos, G. Savard, A system architecture for autonomous demand side load management in smart buildings, *IEEE Transactions on Smart Grid* 3 (4) (2012) 2157–2165.
- [6] K. Margellos, S. Oren, Capacity controlled demand side management: A stochastic pricing analysis, *IEEE Transactions on Power Systems* 31 (1) (2016) 706–717.
- [7] S. Rahim, N. Javaid, A. Ahmad, S. A. Khan, Z. A. Khan, N. Alrajeh, U. Qasim, Exploiting heuristic algorithms to efficiently utilize energy management controllers with renewable energy sources, *Energy and Buildings* 129 (2016) 452 – 470.
- [8] D. Caprino, M. L. D. Vedova, T. Facchinetti, Peak shaving through real-time scheduling of household appliances, *Energy and Buildings* 75 (2014) 133 – 148.
- [9] G. L. Doorman, Capacity subscription: solving the peak demand challenge in electricity markets, *IEEE Transactions on Power Systems* 20 (1) (2005) 239–245.
- [10] T. Logenthiran, D. Srinivasan, T. Z. Shun, Demand side management in smart grid using heuristic optimization, *IEEE Transactions on Smart Grid* 3 (3) (2012) 1244–1252.
- [11] L. Suganthi, A. A. Samuel, Energy models for demand forecasting: A review, *Renewable and Sustainable Energy Reviews* 16 (2) (2012) 1223–1240.

-
- [12] L. G. Swan, V. I. Ugursal, Modeling of end-use energy consumption in the residential sector: A review of modeling techniques, *Renewable and Sustainable Energy Reviews* 13 (8) (2009) 1819–1835.
- [13] K. Ahmed, M. Ampatzis, P. Nguyen, W. Kling, Application of time-series and artificial neural network models in short term load forecasting for scheduling of storage devices, in: *Power Engineering Conference (UPEC), 2014 49th International Universities, 2014*, 1–6.
- [14] R. K. Jain, K. M. Smith, P. J. Culligan, J. E. Taylor, Forecasting energy consumption of multi-family residential buildings using support vector regression: Investigating the impact of temporal and spatial monitoring granularity on performance accuracy, *Applied Energy* 123 (2014) 168–178.
- [15] R. Subbiah, K. Lum, A. Marathe, M. Marathe, Activity based energy demand modeling for residential buildings, in: *Innovative Smart Grid Technologies (ISGT), 2013 IEEE PES, 2013*, 1–6.
- [16] J. Massana, C. Pous, L. Burgas, J. Melendez, J. Colomer, Short-term load forecasting in a non-residential building contrasting models and attributes, *Energy and Buildings* 92 (2015) 322–330.
- [17] H. Zareipour, A. Janjani, H. Leung, A. Motamedi, A. Schellenberg, Classification of future electricity market prices, *IEEE Transactions on Power Systems* 26 (1) (2011) 165–173.
- [18] H. Zareipour, D. Huang, W. Rosehart, Wind power ramp events classification and forecasting: A data mining approach, in: *2011 IEEE Power and Energy Society General Meeting, 2011*, 1–3.
- [19] D. Cluwen, Demand response and storage for demand side management in smart buildings, Internship report, University of Twente and Polytechnique Montreal (April 2014).
- [20] M. Kuzlu, M. Pipattanasomporn, S. Rahman, Hardware demonstration of a home energy management system for demand response applications, *IEEE Transactions on Smart Grid* 3 (4) (2012) 1704–1711.
- [21] Historical climate data, <http://climate.weather.gc.ca>, [Government of Canada; accessed July-2016].
- [22] N. V. Chawla, *Data Mining for Imbalanced Datasets: An Overview*, Springer US, Boston, MA, 2010, 875–886.
- [23] T. E. Dielman, A comparison of forecasts from least absolute value and least squares regression, *Journal of Forecasting* 5 (3) (1986) 189–195.